International Journal of Nanomedicine

Dovepress
Taylor & Francis Group

Open Access Full Text Article

ORIGINAL RESEARCH

Hyaluronic Acid-Based Hybrid Nanoparticles as Promising Carriers for the Intranasal Administration of Dimethyl Fumarate

Carla Serri[1], Miriam Piccioni[2], Vincenzo Guarino[3], Pamela Santonicola[2], Iriczalli Cruz-Maya[3], Stefania Crispi[2], Massimiliano Pio Di Cagno[4], Luca Ferraro[5], Alessandro Dalpiaz[6], Giada Botti[6], Paolo Giunchedi[1], Giovanna Rassu[1], Elisabetta Gavini[1]

[1]Department of Medicine, Surgery and Pharmacy, University of Sassari, Sassari, Italy; [2]Institute of Biosciences and Bio-Resources, National Research Council (CNR-IBBR), Naples, Italy; [3]Institute of Polymers, Composites and Biomaterials, National Research Council of Italy, Naples, Italy; [4]Department of Pharmacy, University of Oslo, Oslo, Norway; [5]Department of Life Sciences and Biotechnology, University of Ferrara and LTTA Center, Ferrara, Italy; [6]Department of Chemical, Pharmaceutical and Agricultural Sciences, University of Ferrara, Ferrara, Italy

Correspondence: Giovanna Rassu, Department of Medicine, Surgery and Pharmacy, University of Sassari, Sassari, Italy, Email grassu@uniss.it

Purpose: Dimethyl fumarate (DMF), the first-line oral therapy for relapsing-remitting multiple sclerosis, is rapidly metabolized into monomethyl fumarate. The DMF oral administration provokes gastrointestinal discomfort causing treatment withdrawal. The present study aimed to develop an innovative formulation for DMF nasal administration. Lipid-polymer hybrid nanoparticles (LPNs) were developed to improve DMF stability, limiting gastrointestinal side effects and increasing brain bioavailability by nose-to-brain targeting application.

Methods: DMF-loaded and unloaded LPNs with or without hyaluronic acid (HA) were prepared using the nanoprecipitation via magnetic/mechanical stirring technique. Particle morphology and surface properties were evaluated; drug content, viscosity, and mucoadhesion were determined. Physico-chemical stability of LPNs and DMF in the LPNs was also explored. In vitro DMF permeation experiments were performed utilizing the PermeaPad®. The cytotoxicity and cellular uptake studies were performed using RPMI 2650 and SK-N-BE2 cell lines. DMF nose-to–brain delivery was evaluated by intranasally administering DMF-loaded LPNs to rats.

Results: LPNs with average sizes of 120–250 nm and a negative zeta potential −17.3 to −43 mV were obtained, primarily influenced by the presence of HA. HA assured drug stability up to 60 days and promoting the in vitro permeation of DMF compared to the free-DMF. HA greatly improved the viscosity and mucoadhesive properties. LPNs with and without HA did not exhibit any cytotoxicity and showed a rapid cell uptake starting from 15 min to 2 h with a best internalization after 1 h of treatment in both epithelial and neuronal cell lines. Nasal administration of DMF-loaded LPNs allowed to quantify up to about 12 µg/mL of DMF in the rat cerebrospinal fluid.

Conclusion: The results highlight the role of HA in improving LPNs properties and performance as carrier of DMF for nasal administration. In particular, LPNs appear able to enter neurons and monolayers of epithelial cells, allowing to promote the nose-to-brain DMF delivery.

Keywords: hyaluronic acid, lipid and polymeric nanoparticles, nasal administration, nose-to-brain delivery, dimethyl fumarate, cell uptake

Introduction

Multiple sclerosis (MS) is a neurodegenerative disorder which affects the central nervous system (CNS). It is characterized by autoimmune-mediated demyelination of axons.[1] The disease is typically classified into four phenotypes: relapsing-remitting MS (RRMS), primary progressive MS, secondary progressive MS (SPMS), and progressive relapsing MS.[2] The etiology of MS is multifactorial, likely involving both genetic susceptibility and environmental factors, such as

Received: 30 July 2024
Accepted: 14 December 2024
Published: 4 January 2025

Graphical Abstract

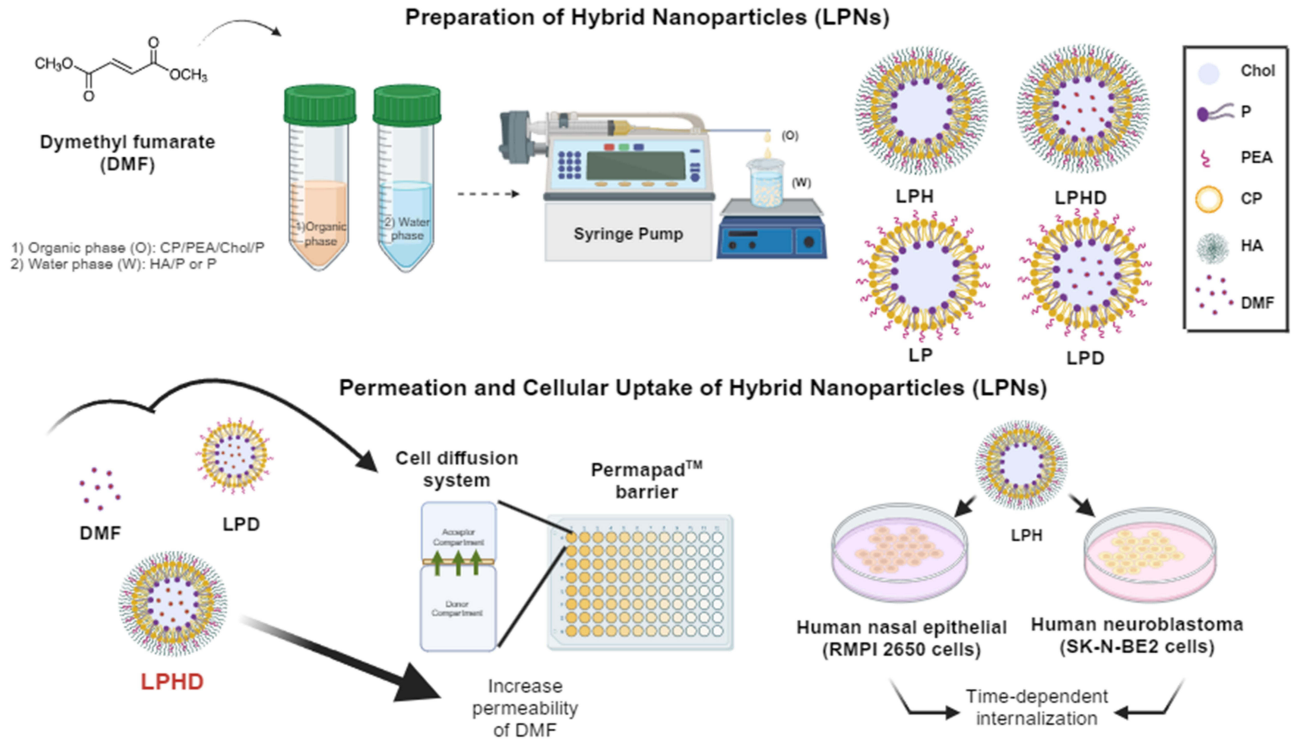

viral infections and vitamin D deficiency, which contribute to its pathogenesis.[3,4] Dimethyl fumarate (DMF) (commercial product Tecfidera®) is a prodrug, which is currently approved by both the FDA and the EMA as a first-line oral therapy for relapsing-remitting MS (RRMS).[1] After oral administration of Tecfidera®, DMF is quickly metabolized by esterase enzymes into its active metabolite, monomethyl fumarate (MMF).[5,6] The DMF is associated with a favorable safety profile; however, it may induce certain adverse reactions. The most prevalent side effects include gastrointestinal complaints and abdominal pain, typically observed within the first year of treatment. Notably, gastrointestinal disorders have been reported in 43% of patients, along with flushing and lymphopenia, leading to treatment discontinuation within the first three months.[7] A significant concern is the development of lymphopenia, which can vary from moderate to severe and, if prolonged, may result in multifocal leukoencephalopathy. Furthermore, DMF treatment alters various immune cell populations. Numerous clinical studies have been conducted to identify individuals at elevated risk and to establish novel strategies aimed at minimizing the occurrence of immune-related adverse reactions.[8] Therefore, improving the stability and bioavailability of DMF is crucial, and strategies employing nanocarrier systems or alternative administration routes present promising solutions. Recent studies have highlighted that innovative formulations such as solid lipid nanoparticles (LNs), nanostructured lipid carriers, and polymeric nanoparticles (NPs)[9–11] can enhance DMF uptake in the brain.[12,13] The intranasal (IN) route emerges as a potential strategy, offering the advantages of mitigating gastrointestinal side effects and enhancing patient adherence, thus providing a more tolerable and effective treatment option.[14] This route allows for rapid drug action, avoids first-pass metabolism, and enables direct brain delivery.[15] The nasal mucosa's high permeability, through both intracellular and paracellular pathways, facilitates direct drug transport to the brain,[14–16] with the olfactory and trigeminal nerves providing direct access to brain tissue.[17] It has been shown that nanoparticles, which range in size from 100 to 700 nm, can be internalized by the cell of the nasal epithelium.[18]

In this work, lipid-polymer hybrid nanoparticles (LPNs) have been developed as DMF carriers for IN administration; LPNs merge the advantages of lipids with the ones of hydrophilic polymers. NPs, indeed, are highly valued for their robust structural integrity, stability during storage, and controlled release capabilities, especially for poorly soluble

lipophilic compounds belonging to BCS class II/IV.[19] LNs have superior biocompatibility and have long been regarded as optimal drug delivery vehicles.[20,21] They present significant limitations due to their rapid clearance by the reticuloendothelial system (RES). Additionally, when the drugs are loaded into LNs, their bioavailability is often jeopardized due to high binding affinity to the lipid matrix or stabilizing agents within the formulation, which can hinder the release of the drug. In some cases, polyethylene glycol has been successfully used in liposomal formulations to reduce RES clearance, thereby enhancing bioavailability.[22,23] This approach was also successful for LNs.[24] Lipid-polymer hybrid nanoparticles have shown improved physical stability and great biocompatibility, attributed to their distinctive two-part structure.[25] Building on this promising finding, the purpose of this research was to develop new lipid-polymer hybrid nanoparticles (LPNs) with or without hyaluronic acid (HA) containing DMF suited for IN administration. These were produced by nanoprecipitation magnetic/mechanical stirring technique using phosphatidylcholine (CP), palmitoylethanolamide (PEA), cholesterol (Chol), poloxamers (P), and optionally hyaluronic acid (HA), with selected concentration. PEA is an endogenous fatty acid mediator synthesized from membrane phospholipids by N–acyl phosphatidylethanolamine phospholipase Lorìa et al demonstrated the effects of PEA on animals suffering from multiple sclerosis (MS). Their results suggest that PEA due to the anti-inflammatory effects may effectively combat neurodegeneration, demyelination, inflammation, and autoimmune reactions in animal models of MS.[26]

HA, a naturally occurring anionic polysaccharide, has attracted significant research attention for anti-inflammatory /antitumor-targeted delivery since it is biocompatible and non-immunogenic and can specifically bind CD44 and RHAMM receptors, which are overexpressed in many forms of inflammations and cancer.[27–29] A recent work by Vasvani et al demonstrated the efficacy of HA for widespread applications in drug delivery, the ability to enhance drug penetration and prolonged formulation retention time due to mucoadhesive properties.[30,31] The combination of PEA and HA in the formulation is very attractive for IN administration because of the characteristics described. Poloxamer, an amphiphilic copolymer of poly(propylene oxide) (PPO) and poly(ethylene oxide) (PEO) blocks, was selected for its membrane interaction, repair properties, biocompatibility, and mucoadhesive characteristics.[26] It also binds hyaluronic acid (HA) chains to create a cross-linked system, elevating strength and drug-loading capacity.[27,28]

The present study focused on characterizing the physicochemical properties of the LPNs, including size, surface charge, drug content in dispersions, morphology, viscosity, and mucoadhesion to evaluate their suitability as IN delivery system. We conducted thermal analyses utilizing differential scanning calorimetry (DSC) to explore the interactions between lipids, polymers and DMF. The physical stability of the formulations by monitoring size trends at 4°C and the chemical stability of DMF, loaded in LPNs at 4°C were evaluated. To investigate the efficacy of formulation to enhance DMF permeation, studies were performed using PermeaPad® barriers set in phosphate buffer solutions as the acceptor medium, with the permeated DMF was quantified via spectrophotometric assay. In addition, cytotoxicity was assessed in vitro, and cellular uptake of LPNs was investigated using RPMI 2650 and SK-N-BE(2). RPMI 2650 are cells derived from squamous cell carcinoma of the human nasal septum that are widely used for nasal drug delivery studies.[32] SK-N-BE(2) are human neuroblastoma cells with neuronal morphology that are commonly used as models for research in neuroscience.[33] Finally, preliminary experiments were designed to evaluate in vivo the rat nose-to–brain delivery of DMF, following the nasal administration of the LPNs.

Materials and Methods

Materials

Dimethyl fumarate (purity 97%) (DMF), Poloxamer F407 (P) (Poly (ethylene glycol)-block-poly (propylene glycol)-block poly (ethylene glycol) mucin (mucin from pig stomach type II) and Nile Red (NR) were purchased by Sigma-Aldrich from Merck (Milan, Italy). Alginate (Protanal LF 120 LS, FMC Corporation) was obtained by FM ByoPolymer (Bergamo, Italia). Palmitoylethanolamide 95% (PEA) and Cholesterol (Chol) was obtained by WVR (Milan, Italy). Lipoid S 100 was gifted by Lipoid GmbH (Ludwigshafen, Germany) (CP) and Hyaluronic acid sodium salt (HA) with a molecular weight of 799.74 kDa by BioChemical Fluka. Acetonitrile, Ethanol, basic sodium phosphate (Na_2HPO_4), sodium chloride (NaCl) and potassium chloride (KCl) were obtained by Sigma-Aldrich (Milan, Italy). The pure water

 https://doi.org/10.2147/IJN.S481917

was prepared by a MilliQ R4 system (Millipore, Milan, Italy). Male Sprague-Dawley rats (200–250 g) were purchased from Charles River laboratories (Calco, Italy).

Cell Culture

All the culture media and supplements were purchased from Euroclone (Euroclone SpA, Pero (MI), Italy). Human neuroblastoma cell line, SK-N-BE(2) (SK) were purchased from the American Type Culture Collection (CRL-2271, ATCC, Manassas, Virginia, USA). Human nasal septum carcinoma RPMI 2650 (RPMI) were purchased from the American Type Culture Collection (ATCC CCL-30) by Dr Tonazzini (Nanoscience Institute-CNR, Italy) and send to our lab after signing a Transfer Agreement. Cell lines were maintained at 37°C in a 5% CO_2 humidified incubator in either RPMI-1640 medium (SK) or MEM Medium (RPMI) with 10% fetal bovine serum (FBS), glutamine (2 mm), sodium pyruvate and antibiotics (0.02 IU/mL penicillin and 0.02 mg/mL streptomycin). All cell lines cells were routinary screened for absence of mycoplasm.

Preparation of LPNs

Unloaded and DMF-loaded LPNs were prepared using a nanoprecipitation magnetic/mechanical stirring method by using the syringe pump (KDS 100 legacy syringe pump-230V, series 100, by Sigma-Aldrich, Milan, Italy). Briefly, weighted amounts of CP, PEA, Chol and P in the weight ratio 3:1:2:2 were dissolved in 5 mL of ethanol (organic phase, O) by stirring for 45 min to 50°C. The organic phase (O) was forced through the needle of a syringe (inner diameter: 11.99 mm) at 333.3 μL/min flow rate[34] and dropwise into 10 mL of an aqueous phase (W) containing P with or without HA, under magnetic stirring. DMF was added to the organic phase to prepare loaded LPNs. The composition and acronyms of the various LNPs were shown in Table 1.

Obtained LPNs were stirred for 5 h until the complete ethanol evaporation, then, filtered by regenerated cellulose syringe filter (pore size: 0.45 μm, filter size: 25 mm, AlfaTech, Genova, Italy) and stored at 4°C. The reproducibility of the preparation method was assessed working in triplicate. LPNs were used to obtain the nanoparticle dispersion.

Characterization of LPNs

Particle Size, Polydispersity Index, and Zeta Potential

The mean diameter and size distribution of LPNs were determined by photon correlation spectroscopy (PCS) using a Coulter N5 (Beckman Coulter, Miami, USA). All samples were diluted in filtered Milli-Q water (0.22 μm pore size, polycarbonate filters, MF-Millipore, Microglass Heim, Italy) and analyzed with the detector at 90°. The polydispersity index (PDI) was used to evaluate the particle size distribution.

Zeta potential (ZP) was measured with a Zetasizer Nano ZS (Malvern Instruments, Malvern, UK) on a 100 μL of LPNs suspended in Milli-Q water at room temperature.

The results were expressed as mean ± standard deviation (SD) of three measures (n = 3).

Table 1 Composition (mg) and Acronyms of the Different LPNs

Acronym	O (mg)				W (mg)		
	CP	PEA	Chol	P	DMF	HA	P
LP	200	100	150	150	–	–	0.05
LPD	200	100	150	150	40	–	0.05
LPH	200	100	150	150		30	0.05
LPHD	200	100	150	150	40	30	0.05

Particle Size Stability

The physical stability of LPNs was studied in terms of the trend of the mean hydrodynamic diameter when stored for 30 days at 4°C. The results are average values obtained from at least three independent measurements.

Morphology

Particle morphology was studied via transmission electron microscopy (TEM, FEI Tecnai G12 Spirit Twin, Eindhoven, The Netherlands), equipped with a LaB 6 source and a FEI Eagle 4k CCD camera. The voltage acceleration was set at 120 kV. The sample was prepared by collecting 100 µL of ultra-dilute LPNs with different composition (eg, LPH, LPHD, LP or LPD) in water onto copper TEM grids (300 meshes, 3 mm diameter).

Thermal Properties

The heat exchanged in the phase transitions was determined by a differential scanning calorimeter (DSC) (Discovery DSC, TA Instruments, Delaware, USA), by a ramp from −20°C to 250°C, with a heating rate of 10°C/min. Tests were conducted for different LPNs, starting from highly concentrated particle dispersion, gently dried overnight under hood to remove liquids in excess, until a powder sample (1.5–2 mg in weight) is obtained. Tests were preliminary assessed also on single components – ie, PEA, Chol, P, HA and DMF – used as controls to verify, case by case, the presence in the LPNs.

Viscosity Determination

The LPNs viscosity behavior was determined in a rotational viscosimeter (Alpha-L, Fungilab, Barcelona, Spain) using the "spindles L1 and L2" at constant rotation speed of 100 rpm at 37°C. Indeed, measurements were made on 20 mL of the LPNs and HA solution (3 mg/mL) as comparison. The results were expressed as mean ± standard deviation (SD) of three measures (n = 3).

In vitro Mucoadhesion Test

The in vitro mucoadhesive strength was evaluated using a regenerated cellulose membrane by a modified precision balance.[35] The test was conducted as previously reported by Lombardo et al substituting the pig nasal mucosa with the synthetic membrane.[36] The membrane (diameter = 1.5 cm) was wetted, to simulate the nasal mucosa, with artificial nasal mucus.[36] LPNs (100 µL) were tested. Further, HA solution (100 µL, 3 mg/mL, viscosity of 238 ± 1.8 cP) was analyzed as comparison; sodium alginate solution (100 µL, 3 mg/mL, viscosity of 9.6 ± 0.4 cP), was tested as the positive control. The mucoadhesive properties were expressed as stress measurement (Pa, mean ± SD, n = 5).

Drug Content Determination and Time Stability

The total drug in LPHD and LPD was measured after preparation, and the DMF chemical stability for 30 days at 4°C was assessed. Samples were analyzed at each predetermined time point (0, 7, 14, 23, 30 days). Briefly, 100 µL of LPHD or LPD was mixed with 9.90 mL of acetonitrile and gently stirred for 30 min at room temperature and sonicated for 2 min at 35 hz to dissolve the particles so that all the DMF could be dissolved in the medium.[37] The obtained solution was analyzed by HPLC, consisting of two ProStar 210 pumps, a ProStar 410 autosampler and a DAD Varian 330 detector (Palo Alto, CA, USA). The chromatographic separation was performed on Hypersil C18, 150 mm × 4.6 mm, 5 µm of particle size (Thermo Fisher Scientific Milan, Italy), preceded by (2 cm × 4.0, 5 mm) guard column. The mobile phase consisted of filtered water (0.22 µm nylon membrane filter and pH adjusted to 2.6 using phosphoric acid), and methanol (50:50, v/v) isocratically eluted at a 1.5 mL/min flow rate at room temperature. The injection volume was 10 µL, and the analysis time was 4 min per sample. Peak areas were measured at 210 nm. Concentrations of the analyte were calculated by standard curve interpolation. The linearity of the response was 10–500 µg/mL concentration range ($y = 195550x + 1141197$, $R^2 = 0.999$). The total drug in LPHD and LPD was calculated and reported as percentage. Drug content (DC%), as percentage, was calculated by using the following Equation 1.[38]

$$DC\ \% = 100 * \frac{amount\ of\ DMF\ in\ LPNs}{theoretical\ amount\ of\ DMF\ used} \quad (1)$$

 https://doi.org/10.2147/IJN.S481917

In vitro Permeation Study

In vitro permeation studies were performed utilizing high-through put 96-well PermeaPad® plate (InnoMe GmbH, Espelkamp, Germany).[39] The PermeaPad® represents a rapid, yet precise, and efficient approach to investigate drug permeability of enabling formulations.[40] It consists of two regenerated cellulose membranes enclosing a layer of dry phospholipids between them, having a thickness of approximately 0.10 mm. Once hydrated, this barrier forms a liposomal gel that, in structure and composition, reassembles a cellular monolayer and accounts for paracellular drug transport. A mixture of PBS pH 7.4 (v/v) was used as the acceptor solution (400 µL).[34] The donor (200 µL) compartments were filled using DMF solubilized in PBS (0.15 mg/mL) and LPD and LPHD. After filling both the acceptor and donor compartments, the plates were incubated in an orbital shaker–incubator (ES-20, Biosan, Riga, Latvia, LV) at 25°C and 200 rpm for 5 h, respectively. In the experimental setup, samples were assessed both in the presence and absence of mucin 5% (w/v). Precisely, 20 µL of purified mucin dispersion was deposited onto the surface of a PermeaPad-® barrier. This was followed by an equilibration period, during which the plate was subjected to orbital shaking at 100 rpm for 10 min to facilitate uniform distribution of the mucin. Subsequently, the plate was stored at refrigeration temperatures overnight to promote the solidification of the mucin layer. Samples (100 µL) were taken from the acceptor after incubation for 5 h. Three replicates were assessed for each sample. Assuming neglectable lag-time and steady state conditions, the Papp (apparent permeability, cm/sec) of the investigated drugs was calculated by Equation 2.

$$P_{app} = \frac{Q}{t * S * C_d} \tag{2}$$

where Q is the accumulated mass, t is the time and S is the permeation surface (0.13 cm^2). For some selected experiments, sampling was performed at 1 h interval times for 5 h.[39]

For DMF quantification, the samples were directly transferred upon withdrawal to a UV-transparent 96-well micro-liter plate (Corning Inc., Kennebunk, ME, USA), and the absorbance was measured at λ = 253 nm on a microplate spectrophotometer (SpectraMax 190, Molecular Devices Inc., Sunnyvale, CA, USA). Standard solutions (concentration range: 1–0.025 mg/mL) were measured on the same plate, and blank absorption (PBS 7.4 v/v) was deducted from all measurements' UV-Vis spectra.

Cytotoxicity Assay

To detect the safer concentration of LP and LPH, cells were plated in 96-well plates. SK were seeded at 9.5×10^3 cells/well while RPMI at 1.5×10^4 cells/well. The day after, cells were treated with different concentrations of LP or LPH diluted in culture medium. For each cell line, both formulations were tested at 10, 30 and 50 µg/mL concentrations for 24 and 48 h. Untreated cells were used as control. Subsequently, cells were collected and counted with Trypan Blue solution (Sigma-Aldrich, St. Louis, MI, USA). Cell viability was also evaluated by MTT assay (Thiazolyl Blue Tetrazolium Bromide; Sigma-Aldrich, St. Louis, MI, USA) according to the manufacturers' instructions. For the MTT assay, the absorbance was recorded on a microplate reader at a wavelength of 570 nm (VICTOR Multilabel Plate Reader; PerkinElmer, Inc., Waltham, MA, USA). All experiments were performed in biological triplicate.

Cellular Uptake by Fluorescence Microscopy

Fluorescent LPNs (F-LP and F-LPH) were prepared by adding 1 mg/mL of the fluorescent Nile Red (NR) (Merck KGaA, Darmstadt, Germany) to the organic phase containing CP/PEA/Chol and P, with or without HA. NR was chosen since it is fluorescent only in a hydrophobic environment with an intensity related to the hydrophobicity of the solution.[34] The recovered nanoparticle dispersion was centrifuged and washed three times to remove non-encapsulated NR (10,000 rpm, 10 min). Briefly, to evaluate the cellular uptake of LP and LPH, 1.5×10^4 RPMI cells were seeded on 96-well plates and 16 h after seeding were treated with 10 µg/mL of F-LP and F-LPH. The particles were incubated with cells for various timespans, ranging from 15 min to 3 h. Untreated cells were used as control. After treatments, cells were washed with 1× PBS (Microgem, Naples Italy) and then fixed with 4% paraformaldehyde for 10 min at room temperature. Then, cells were rinsed six times with PBS and permeabilized with 0.1% Triton X 100 (Merck KGaA) for 10 min at room temperature. After three washes in PBS, cells were stained

with phalloidin conjugated to Alexa Fluor 488 (Invitrogen, Waltham, MA, USA) to stain F-actin. The phalloidin was diluted 1:200 in 0.1% Triton X-100 and 1% BSA and incubated 1 h at room temperature in the dark. Cells were rinsed again three times with PBS and nuclei were counterstained with DAPI diluted 1:100 (Invitrogen, Waltham, MA, USA), for 5 min at room temperature in the dark. After choosing the best time for internalization, this time treatment was used to perform the experiments in SK and RPMI cells. Cells were seeded on 96-well plates at concentration of 1.5×10^4 for both cell lines; 16 h after seeding, cell lines were treated with 10 μg/mL of F-LP and F-LPH for 1 h and stained as above. Microscopy image acquisition was performed using a fluorescence microscope, and fluorescence was quantified with Leica Application Suite X software (Leica, Milan, Italy). All experiments were performed in biological triplicate. Quantification of the F-LP and F-LPH fluorescence into cells was performed using ImageJ (https://imagej.net/ij/).

In vivo Nasal Administration of DMF-Loaded LPNs

Preliminary experiments were performed in rats to evaluate the possible nose-to-brain of DMF after the nasal administration of DMF-loaded LPNs. To this aim, DMF was administered via intranasal route at a dose of 1 mg/kg (about 0.2 mg/rat) as loaded in LPHD formulation to a group (n = 4) of male Sprague-Dawley rats fasted for 24 h, anesthetized, and laid on their back. Specifically, rats received in each nostril 50 μL of the LPHD formulation (DMF content 2 mg/mL). The nasal administration was performed using a semiautomatic pipet attached to a short polyethylene tubing. The tubing was inserted approximately 0.6–0.7 cm into each nostril. After the administration, cerebrospinal fluid (CSF) samples (50 μL) were serially collected at fixed time points from each rat by using the cisternal puncture method described by van den Berg et al.[41] In particular, a single needle stick, which allowed the collection of serials CSF samples that are virtually blood-free, was used for this procedure,[42] collecting a maximum total volume of about 100 μL of CSF for each rat (ie three 30 μL samples/rat) during the pharmacokinetic experiments, choosing the time points to allow the restoring of the CSF physiological volume.

The CSF samples (10 μL) were immediately analyzed via HPLC for DMF quantification. The chromatographic apparatus was composed of a modular system (model LC-40D) pump and DAD detector (model SPD-M40, Shimadzu, Kyoto, Japan), including an injection valve with a 20 μL sample loop (model 7725; Rheodyne, IDEX, Torrance, CA, USA). Separations were performed at room temperature on a 5 μm Hypersil BDS C18 column (150 mm × 4.6 mm i.d.; ThermoFisher Scientific Spa Italia Srl, Milan, Italy) in turn protected by a guard column packed with the same Hypersil material. The mobile phase consisted of an isocratic mixture of water and acetonitrile at a ratio of 80:20 (v/v) with a flow rate of 0.8 mL/min. The chromatograms were displayed at 216 nm, and the retention time of DMF at the described condition was 8.2 min. CLASS-VP Software, version 7.2.1 (Shimadzu Italia, Milan, Italy) was used to acquire and process all data.

CSF was simulated using standard aliquots of the balanced solution DPBS without calcium and magnesium in the presence of 0.45 mg/mL bovine serum albumin (BSA).[43,44] A preliminary analysis on a blank rat CSF sample, to verify the absence of interferences during DMF analysis, was performed. The chromatographic precision was evaluated by repeated analysis (n = 6) of the same sample solution containing DMF at a concentration of 50 μM (7.21 μg/mL) dissolved in CSF simulation fluid and was represented by a relative standard deviation (RSD) value of 0.95. A calibration curve of peak areas *versus* concentration in the range 0.3 to 150 μM for DMF (0.04 to 21.62 μg/mL), obtained dissolving the compound in CSF simulation fluid, was generated and resulted linear (n = 8, $r = 0.999$, $p < 0.0001$).

The experimental procedures were approved by the Italian Ministry of Health and were performed in accordance with the European Communities Council Directive of September 2010 (2010/63/EU). According to the ARRIVE guidelines, all possible efforts were made to minimize animal pain and discomfort and to reduce the number of experimental subjects.

Statistical Analysis

The statistical data analysis was performed using GraphPad Prism 9.5.1 software (GraphPad Software, Inc., San Diego, CA, USA). An unpaired *t*-test was performed for the statistical difference between the two treatment groups. Turkey's

multiple comparison tests followed a one-way ANOVA analysis of variance test in case of multiple comparisons. Statistical significance was set at $p < 0.05$.

Results

Preparation and Characterization of LPNs

The nanoprecipitation magnetic/mechanical stirring technique allows the preparation of loaded and unloaded LPNs prepared by self-assembling of different components.

Figure 1 shows selected TEM micrographs of LP, LPD, LPH and LPHD. The images revealed a not perfectly spherical shape (Figure 1A) that is amplified by the synergistic effect of HA and DMF (Figure 1D).

In particular, LPNs show a mean size (Table 2) increase from 118 nm (LP) to 255 nm (LPH) and from 215 nm (LPD) to 249 nm (LPHD), due the presence of HA, without or with DMF loading, respectively. The DMF loading in LPD also increased the mean diameter respect to LP ($p < 0.05$).

Moreover, PDI was about 0.30 for LP; however, it markedly increased up to 1.3 when HA is added (LPH) and decreased to 0.6 after DMF loading (LPHD) as well as the mean diameter ($p<0.05$) (Table 2). Accordingly, ZP was also influenced by HA addition, showing more negative values from −17.3 (LP) to −27.93 mV (LPH). Noteworthy, the presence of DMF loading also decreased ZP values (Table 2), from −17.3 (LP) to −29.02 (LPD) and from −27.93 (LPH) to −43.00 mV (LPHD), due to its peculiar polar behavior.

Furthermore, no significant variations in the size stability along 30 days of LP were observed (Table 3). However, only the LPH and LPHD formulations showed a slight increase in diameter at day 30 ($p < 0.05$).

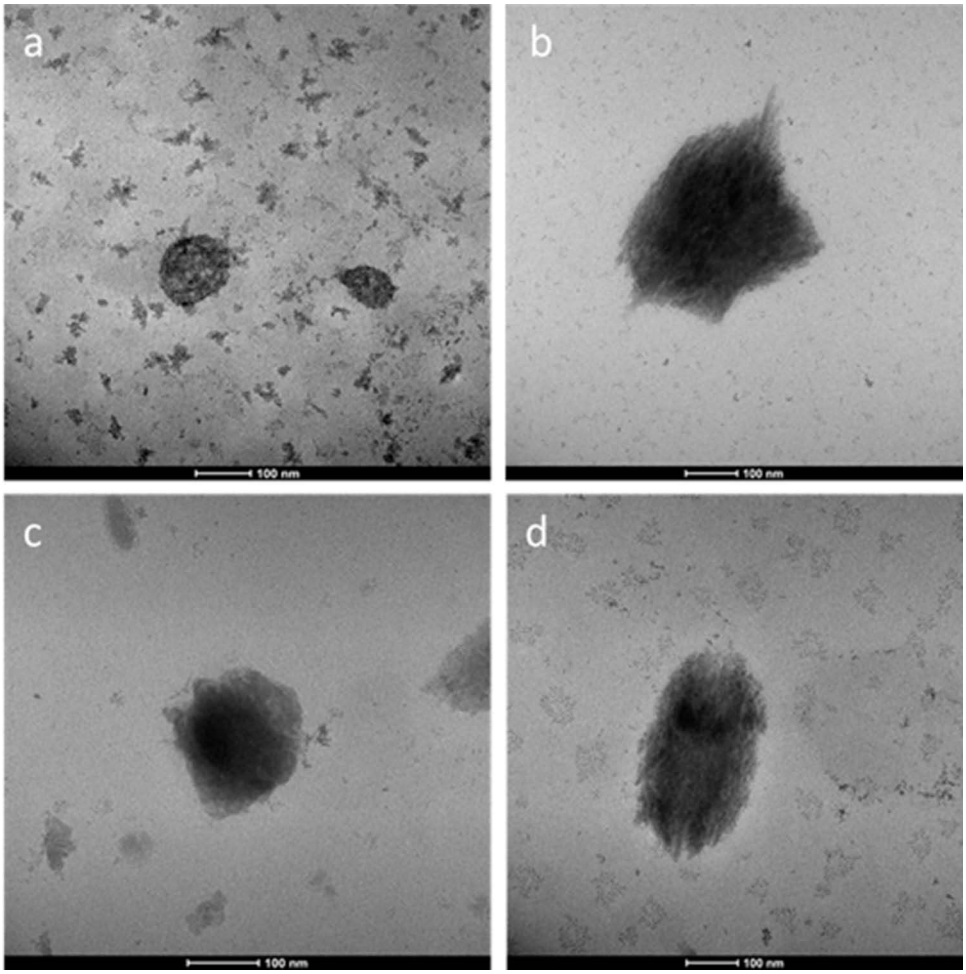

Figure 1 TEM images of LP (**A**), LPH (**B**), LPD (**C**) and LPHD (**D**) (scale bar 100 nm).

Table 2 Size, PDI, ZP and DC of LPNs. Results are Expressed by Mean ± SD *p < 0.05 LP vs LPD; **p < 0.05 LPH vs LPHD; #p < 0.0001 LP vs LPH; $p < 0.05 LPD vs LPHD

Formulations	Particle Size (nm)	PDI	ZP (mV)	DC (%)
LP	118 ± 1.0* #	0.300 ± 0.01* #	−17.3 ± 1.10* #	
LPD	215 ± 1.9* $	0.457 ± 0.04* $	−29.02 ± 0.53* $	65.02 ± 3.4
LPH	255 ± 2.0** #	1.300 ± 0.01** #	−27.93 ± 0.01** #	
LPHD	249 ± 2.9** $	0.600 ± 0.01** $	−43.00 ± 2.30** $	69.82 ± 0.7

Table 3 The Mean Diameter (Nm) ± SD of LPNs, Stored at 4°C for 30 Days *p < 0.05 Day 0 vs Day 30

Formulations	Day 0	Day 10	Day 20	Day 30
LP	118 ± 1.0	154 ± 4.5	111 ± 1.7	116 ±1.3
LPD	215 ± 1.9*	216 ± 3.4	178 ± 2.4	197 ± 3.8*
LPH	255 ±1.6*	267 ± 1.6	229 ± 4.5	272 ± 1.7*
LPHD	249 ± 2.9*	267 ± 1.2	283 ± 3.2	284 ±4.0*

DSC analyses were performed to verify the composition of different LPNs. Figure 2 showed thermograms with characteristic endothermal peaks related to the melting transition of the main components in the different LPNs. In the square (Figure 2B), characteristic peaks of major components were also reported as reference. Characteristic temperatures (Tm) about 60.9°C and 78.5°C related to P and PEA, respectively, were clearly recognized in the thermogram of the LPNs. Meanwhile, characteristic peak of DMF (107.7°C) was recognized in the case of LPD, with a slight down-shift to 105.3°C in the case of LPHD (Figure 2A); it was partially overlapped with the HA peak (103.8°C), slightly shifted in comparison with the characteristic peak of the pure component (102.2°C), probably due to moderate polar interactions among the two components.

As expected LPH and LPHD containing HA showed higher viscosity (183 ± 0.4 and 134 ± 1.3 cP, respectively) than LP (28.63 ± 3.2 cP) and LPD (23.00 ±1.8 cP) ($p < 0.0001$). The viscosity resulted lower than HA solution (3 mg/mL, 238 ± 1.8 cP).

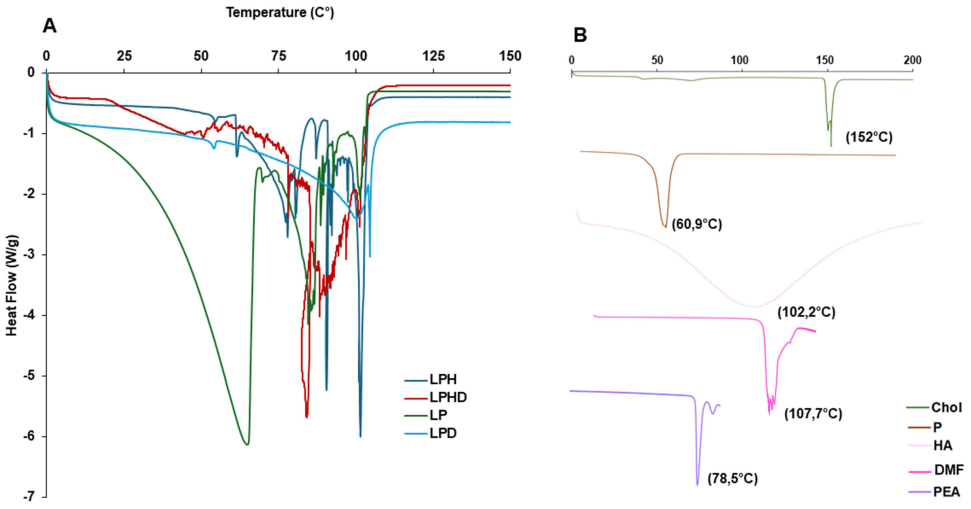

Figure 2 DSC thermograms of LPNs (**A**). In the square, the characteristic peaks of major components (eg Chol (green line), P (brown line), HA (pink line), DMF (violet line), PEA (fuchsia line) (**B**).

https://doi.org/10.2147/IJN.S481917

Figure 3 illustrates the results of the mucoadhesion test expressed as the stress (Pa) required to detach samples from the membrane's surface and compared with the alginate solution. The detachment stress was higher than blank only for LPH and LPHD containing HA ($p < 0.0001$). However, the same formulations showed a detachment stress lower than the alginate solution. The DMF loading significantly decreased the detachment force ($p < 0.0001$).

Drug Content and Time Stability

As shown in Table 2, the DC% is independent on the HA presence: 65% in case of LPD vs 69% of LPHD ($p > 0.05$). However, results on the time stability determination highlighted the protective effect of HA on DMF degradation (Figure 4). In fact, the total amount of DMF was stable in the LPHD up to 60 days ($p > 0.05$), while the total DMF in LPD rapidly decreased from 2.8 mg/mL (65%) to 0.8 mg/mL (20%) after 7 days and since 0.5 mg/mL (12%) after 14 days ($p < 0.05$).

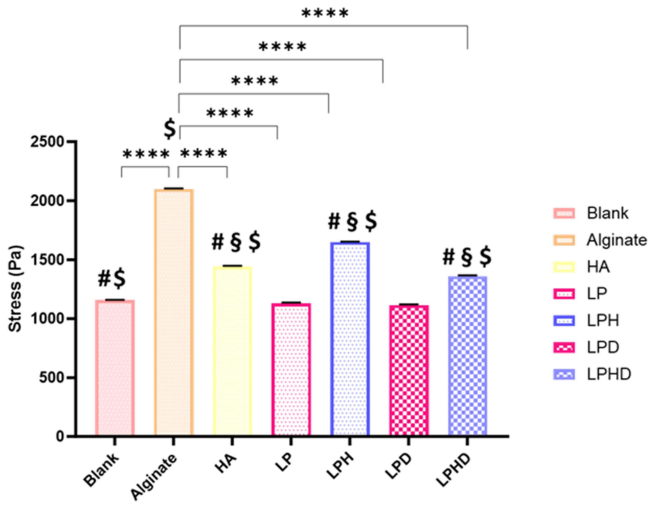

Figure 3 Stress (Pa) needed to detach LPNs, the HA solution and the Alginate solution from membrane saturated with artificial nasal mucus (n = 3). (****$p < 0.0001$ Alginate vs Blank/LPNs; $^{\#}p < 0.0001$ Blank vs LPH/LPHD/HA; $^{\S}p < 0.0001$ LPH vs LPHD; $^{\$}p < 0.0001$ hA vs Blank/Alginate/LPH/LPHD).

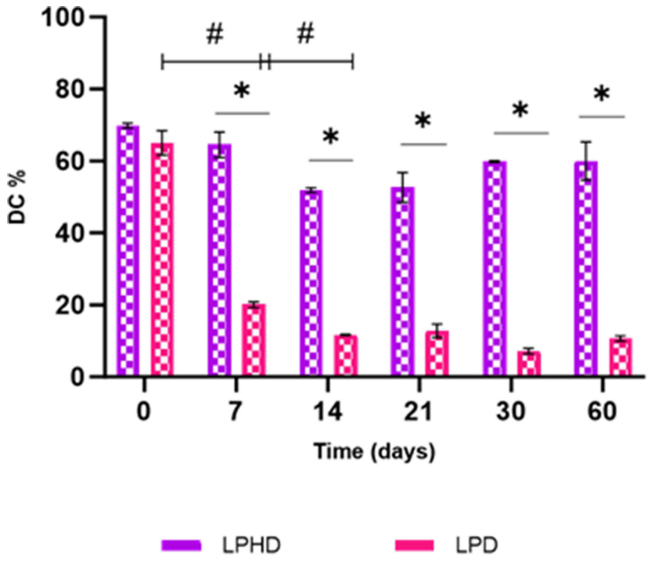

Figure 4 Time stability of LPD and LPHD for 60 days. The results are reported as DC % ± SD (n=3). *$p < 0.001$ LPHD vs LPD; $^{\#}p < 0.01$ LPD t0 vs LPD t7 days and LPD t7 days vs LPD t14 days.

https://doi.org/10.2147/IJN.S481917

In vitro Permeation Study

The in vitro permeation experiments measured the absorption rate of DMF, from LPD, and LPHD into the acceptor medium, both with and without a mucin layer. As shown in Figure 5, the apparent permeability (P_{app}) of free-DMF was significantly lower ($p < 0.05$) compared to that of DMF loaded in LPD and LPHD, irrespective of the mucin layer's presence. The data showed that the apparent permeability (P_{app}) values range from 1.5×10^{-7} cm/s for free-DMF to 1.2×10^{-7} cm/s for free-DMFm, from 2.1×10^{-7} cm/s for LPD to 1.2×10^{-7} cm/s for LPDm, and from 3.1×10^{-7} cm/s for LPHD to 2.5×10^{-7}cm/s for LPHDm. These findings indicate that LNPs enhanced the permeation of DMF across the barrier both in the presence and absence of mucin. Additionally, it is noteworthy that LPHD and LPHDm facilitated greatly drug permeation, although the differences in permeability with and without mucin were not statistically significant ($p > 0.05$). In Figure 6, the flux profile from LPD and LPHD are reported over a time. The data clearly demonstrated that LPD and LPHD, exhibited enhanced flux (ie, slope of the curve) when compared to the free-DMF. Whereas for free-DMF the flux seemed to be quite linear (R^2= 0.995

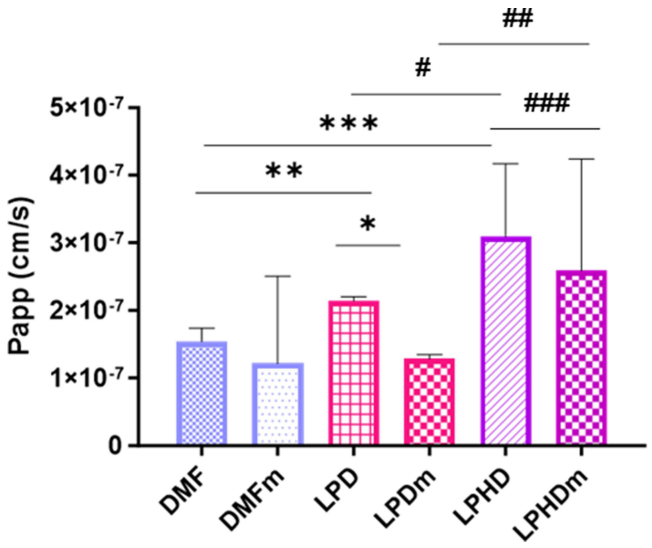

Figure 5 In vitro permeations of free-DMF aqueous solution LPD and LPHD through the PermeaPad barrier over 5 h without and with mucin (DMFm, LPm, LPHm) (n = 3). *p < 0.05; LPD vs LPDm; ###p<0.05 LPHD vs LPHDm; **p < 0.05 DMF vs LPD; #p < 0.05 LPD vs LPHD; ***p < 0.05 DMF vs LPHD; ##p < 0.05 LPDm vs LPHDm.

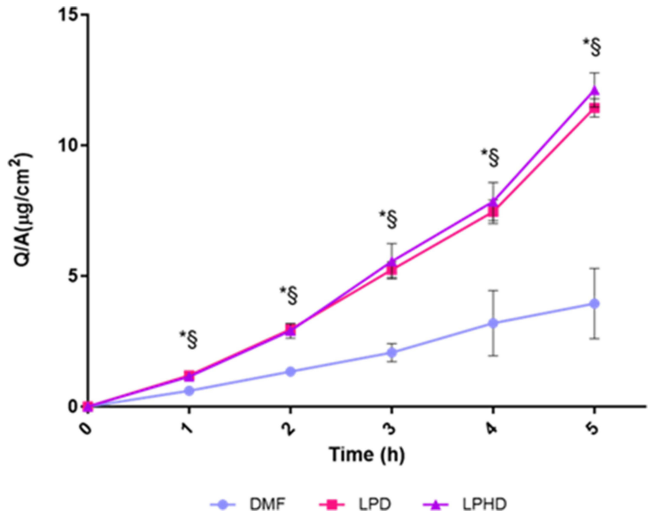

Figure 6 In vitro permeation of free-DMF aqueous solution, LPD and LPHD through PermeaPad® barrier over 5 h (n = 3). *p < 0.0001 DMF vs LPD; §p < 0.0001 DMF vs LPHD. There are no statistical differences between two formulations (p> 0.05 LPD vs LPHD at all time points).

https://doi.org/10.2147/IJN.S481917

of the slope), for both LPD and LPHD the permeation rate seemed to increase overtime, with an average flux of 4.7×10^{-7} µg*cm^2 and 4.9×10^{-7} µg*cm^2 (R^2= 0.968 and 0.967), respectively.

In vitro Cytotoxicity and Uptake Analysis

To evaluate the possibility to use LP and LPH for the nose-to-brain targeted delivery, we used two human cell lines as model for the in vitro studies to simulate the nasal cellular structure: RPMI a cell model of nasal epithelium and SK a neuronal cell model.

To evaluate the ability of LP and LPH to entry into SK and RPMI cell without affecting viability, we first analyzed cell viability by using MTT assay and Trypan blue staining. To this aim, cells were treated with increasing concentrations of LP or LPH for 24 and 48 h (Figure 7). The results showed that the concentration with no effect on cell viability corresponds to 10 µg/mL. In fact, as shown in the figure there are no difference in cell number in treated or in untread cells in both SK and RPMI cells. In addition, we did not observe changes after 24 and 48 h of treatment. This result allowed us to use this concentration the subsequent uptake analysis.

For uptake analysis, we first performed a time course analysis on RMPI cells using fluorescent LP and LPH to identify the shortest time needed to achieve internalization. Cells were incubated with 10 µg/mL of F-LP and F-LPH for different times ranging from 15 to 180 min, then cells were fixed and stained and then analyzed. In Figure 8 are shown

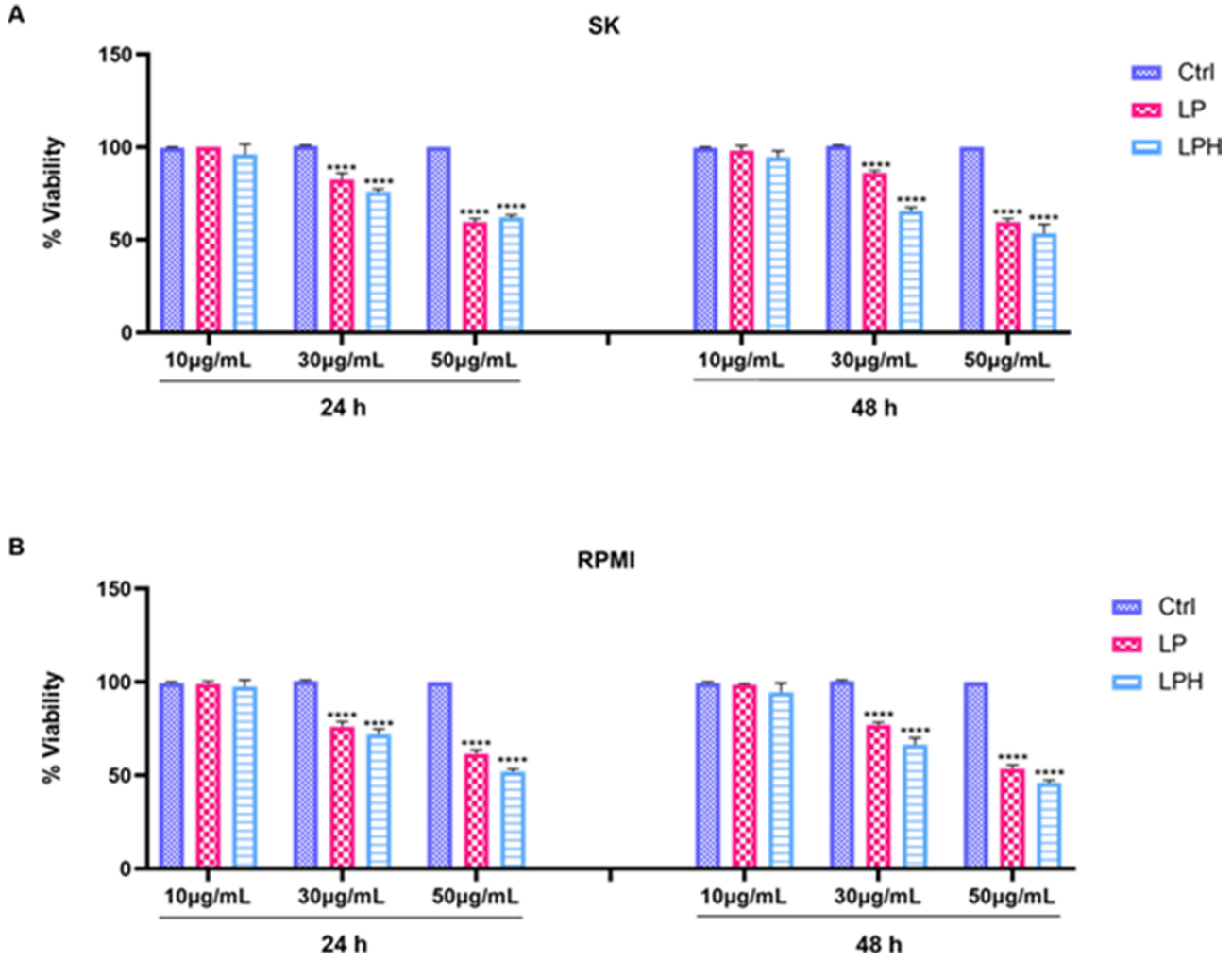

Figure 7 LP and LPH cytotoxicity analysis. SK (**A**) and RPMI (**B**) cells were treated with 10, 30 and 50 µg/mL of LP or LPH for 24 and 48 h. 10 µg/mL resulted from the safest concentration for both cell lines at 24 and 48 h. Untreated cells were used as control (Ctrl). Data are presented as the mean ± standard deviation and are representative of at least three independent experiments (n = 3). **** $p < 0.0001$ vs control.

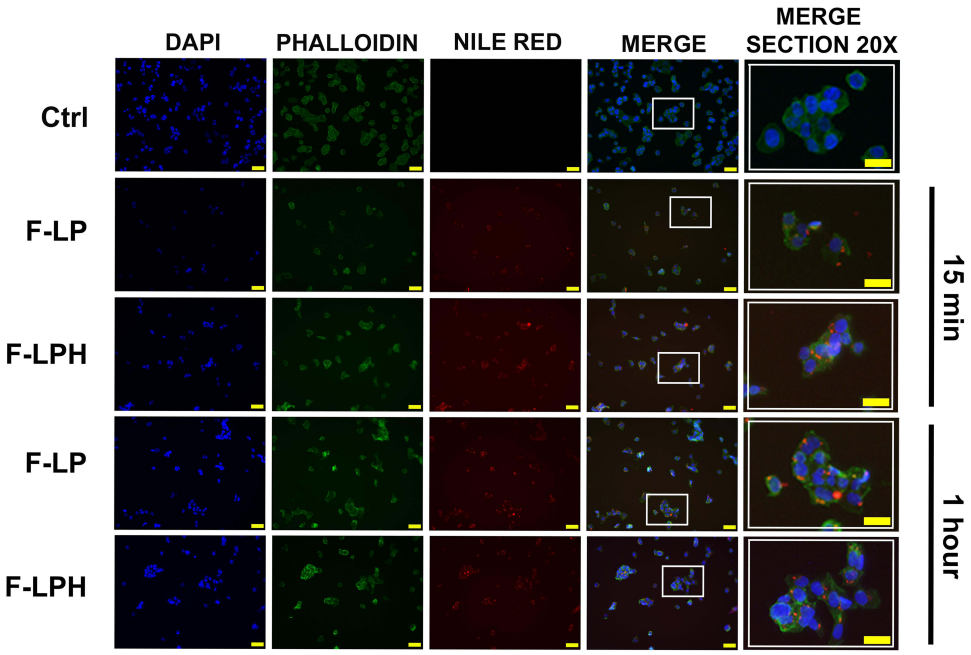

Figure 8 Uptake of F-LP and F-LPH after 15 min and 1 h. RPMI cells were treated with 10 μg/mL of F-LP or F-LPH and internalization was monitored with fluorescence microscopy. RPMI were stained with phalloidin and DAPI (20× magnification). Control indicates untreated cells (Ctrl). For each time analyzed, is shown on the right an enlargement of the white rectangle section from the merge pictures (MERGE SECTION 20X). The yellow bar in each picture corresponds to 50 μm. All data are representative of at least three independent experiments.

the best time of internalization compared to the lower, while all the internalization times are showed in Supplemental Figure 1. F-LP and F-LPH were internalized already after 15 min, and the process increased over the time up to 1 h. At this time there is a clear colocalization of F-actin (green) and fluorescent nanoparticles (red) that indicates a cytoplasmatic localization of both formulations. After this time and up to 3 hours, we observed a progressive reduction of intracellular red fluorescence that could indicate nanoparticle release.

Given that, 1 h treatment resulted the best internalization time, we decided to perform a new experiment on both cell lines. The results (Figure 9A and B) confirmed that the uptake of both formulations occurred after 1 h in both cell lines and showed that both F-LP and F-LPH has a similar cytoplasmatic localization. Analysis of the fluorescent red signals indicated a better uptake of F-LPH in both cell lines (22% in RPMI, 24% in SK) compared to F-LP (12% in RPMI, 14% in SK) (Figure 9C).

In vivo Nasal Administration of DMF-Loaded LPNs

Preliminary experiments were performed in rats to evaluate the possible nose-to-brain of DMF after the nasal administration of LPHD. DMF was administered intranasally at the dose of 1 mg/kg loaded in the LPHD. Figure 10 reports the DMF profile detected over time in rat CSF following the intranasal administration. DMF concentration increased up to 12.52 ± 1.68 μg/mL (C_{max}) within 20 min (t_{max}), then decreased to zero within 150 min from the end of administration.

Discussion

Recent studies have shown that delivery of DMF in nanoparticles results in increased bioavailability after oral administration and improved motor dysfunction;[9,10,12] Pinto et al showed that the inflammatory process and disability progression were reduced by inhalation of DMF encapsulated in SLNs.[45] In the last decade, the IN route has been widely explored as an alternative administration way aimed at systemic or nose-to-brain delivery of drugs to prevent/treat CNS diseases.[46,47] The IN route may be advantageous for the administration of DMF, which causes severe GI side effects when orally administered. Esposito et al proposed DMF-loaded SLNs for IN administration.[48] The present work, thus, aimed to investigate the LPNs for IN administration of DMF.

https://doi.org/10.2147/IJN.S481917

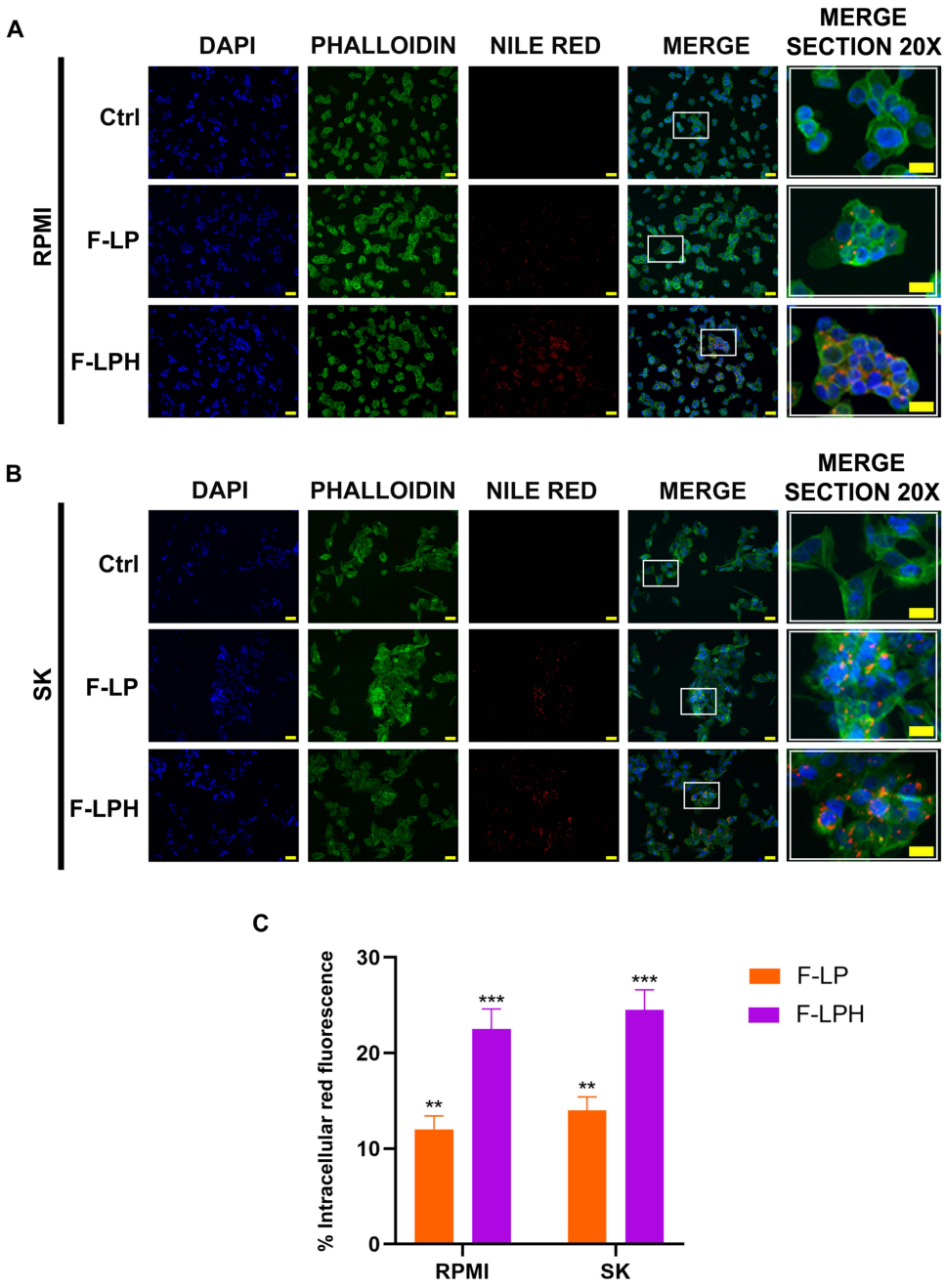

Figure 9 Uptake of F-LP and F-LPH after 1 h treatment. Cytoplasmatic localization of 10 μg/mL F-LP and F-LPH, in RPMI (**A**) and SK (**B**) cells. Microscope fluorescence images of cells stained with phalloidin and DAPI (20× magnification). For each cell line, on the right are shown white rectangle enlargement of sections from the merge pictures (MERGE SECTION 20X). (C) Fluorescence quantization of the intracellular red signals. Red signals have been normalized. Control indicates untreated cells (Ctrl). The yellow bar in each picture corresponds to 50 μm. All data are representative of at least three independent experiments. All data are representative of at least three independent experiments (n=3). **p < 0.01 F-LP vs control, ***p < 0.0004 F-LPH vs control.

The LNPs, with and without HA, were prepared utilizing the nanoprecipitation via magnetic/mechanical stirring technique. This approach is advantageous for its simplicity and rapid execution at laboratory scale, while providing precise control over the formulation settings.[34] The LPNs preparation involved the assembly of CP, PEA to obtain the basic structure, Chol and P to confer rigidity to the nanoparticles, and HA to improve mucoadhesion and increase nanoparticles physical stability. HA chains, indeed, tend to form hydrophobic interactions and hydrogen bonding with CP bilayers and P, respectively, promoting a good stability, in agreement with previous investigations conducted by Zeng

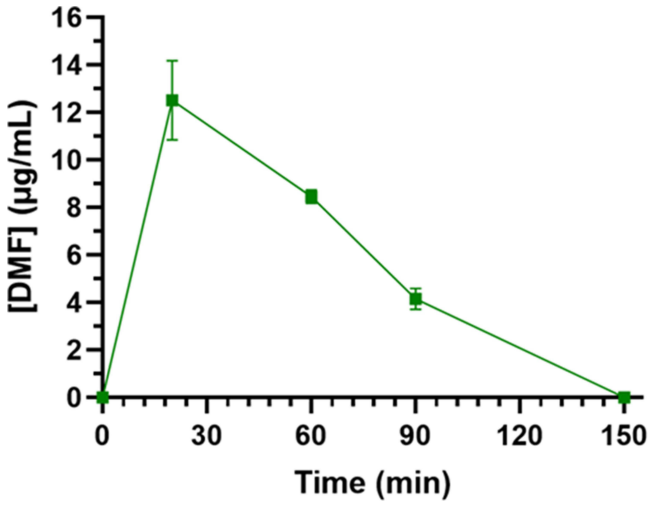

Figure 10 DMF concentrations (µg/mL) detected in rat CSF after intranasal administration of 0.2 mg (1 mg/kg DMF dose) of DMF loaded in LPHD. Data are expressed as mean ± S.E.M. of four independent experiments.

et al[49–51] PEA was included in formulation composition as it may also exert a synergic effect with DMF by combating inflammation, neurodegeneration and demyelination.[26]

The performed studies demonstrated that HA strongly affects the properties of LPNs. In particular, HA determines an increase in size and PDI and makes more negative LPNs surface. HA-containing nanoparticles have a larger size than those without HA, and it is known that a change in solution viscosity affects the size during nanoprecipitation.[51] High molecular weight HA is mainly involved in increasing the viscosity affecting the polydispersity index (PDI).[52] The obtained PDI values suggested a heterogeneous distribution of particle sizes. In fact, the addition of only HA (LPH) resulted in a high increase in PDI, but the presence also of DMF (LPHD) caused a significant decrease in PDI that could be due to an interaction between the two substances, as also evidenced by the results of DSC analysis.

Simultaneous presence of HA and DMF (LPHD) resulted in significantly decreasing ZP values. It is known that a ZP value less than −30 mV guarantees optimal nanoparticle physical stability in dispersion.[53,54] In fact, only a slight increase in size was found after 30 days.

As concerning the drug content, no statistical differences were observed between LPNs. However, DMF content is stable only when HA is included in LPHD as DC% do not change statistically from time 0 to time 30 days, whereas in the case of the LPD, the amount of loaded DMF is dramatically reduced as early as 7 days to as low as 12% after 14 days. Once again HA plays a crucial role in the performance of LPHD: due to the interaction of chains HA crosslinked with the chains of P and CP,[50,51] DMF would be entrapped in the nanoparticles and protected by the hydrolysis. DMF, indeed, is a drug susceptible to hydrolysis and sublimation with low stability along the time.[37,55] Furthermore, as hypothesized from DSC results, HA may form polar interactions with DMF, preventing its release into the surrounding medium, where it degrades.

The combination of nanotechnology with IN administration offers excellent opportunities for the effective systemic and cerebral delivery of different therapeutic agents. It is essential to understand the interactions between nanomaterials and the nasal biological environment to achieve fit drug delivery. Mucociliary clearance is a significant challenge for efficient drug delivery by IN route targeting the brain or systemic circulation, and therefore viscosity and mucoadhesion are key factors in nasal drug delivery.[18,56,57]

The viscosity of the formulations was determined as a parameter required by FDA in the characterization of nasal formulations. LPH and LPHD show higher viscosity than LP and LPD, but lower than HA solution for the involvement of HA in the nanoparticle structure.[58] Although an optimal viscosity range is not reported, a high viscosity is required to ensure a prolonged residence time of the formulation in the nasal cavity.[59]

Same behavior was observed regarding results from the mucoadhesion test: the HA greatly improves the mucoadhesive properties of LPH and LPHD compared to LP and LPD, which showed no significant differences compared to the

https://doi.org/10.2147/IJN.S481917

blank and between each other. Mayol and collaborators demonstrated that the mucoadhesive properties of P are enhanced in the presence of HA.[60] In particular, LPH showed higher mucoadhesion values than LPHD likely because of reduced availability of HA chains to interact with hydrophilic bonds with mucin, being involved in interactions with DMF as previously hypothesized.[56,61] However, LPH shows higher detachment strength than HA solution, as reported by Sepulveda and de Araujo, the presence of P and HA results in increase mucin interactions.[62] Mucoadhesion is crucial for a nasal formulation because it is able to counteract mucociliary clearance by ensuring an increased residence time of the formulation in the nasal cavity and contact with the nasal mucosa at the site of deposition, thus contributing to improved drug absorption.[55]

The in vitro permeation studies also clearly indicated that both LPD and LPHD produced an increment in drug permeation over time compared to the free-DMF. The reason for this increase most likely lies in the higher free drug concentration in the LPNs in comparison to the DMF solution (0.15 mg/mL). What is very remarkable is that the presence of the HA increases even more the permeation of DMF in comparison to LPD. As described earlier, lipid nanocarriers and hydrophilic polymers can increase the free drug fraction of drugs producing a local supersaturation and, therefore, a higher permeation in vitro. This increases the concentration gradient between the donor and the acceptor compartment, thus, promoting a higher drug flux and permeation. Our finding suggests that this might be the mechanism by which the nanocarriers LPHD increases the permeability in vitro.[63] The observed enhancement in drug permeation facilitated by LPD and LPHD underscores their potential efficacy in promoting the intranasal delivery of DMF. In light of this promising permeation profile, it is crucial to evaluate the safety of these LPNs using relevant cellular models. Given that LPNs were developed specifically for drug delivery for the nasal administration, we investigated, in a final set of experiments, the absence of any cytotoxicity on RPMI and SK cell lines usually used for IN delivery and for neuroscience research, respectively.[61,64] LNPs did not exhibit any toxicity to RPMI and SK cells. The results indicate that at 10 µg/mL both formulations do not affect cell viability. In addition, both nanoparticles are able to enter into cells, in both cell lines, in a time-dependent manner with a good internalization evidenced after 1 h and with a better performance of F-LPH, as showed by fluorescence intensity.

The results showed that LPHD have suitable characteristics for the IN administration of DMF and also support the ability of nanoparticles to be internalized into both epithelial and neuronal cells, suggesting their potential ability to promote the nose-to-brain transport of DMF. This hypothesis is supported by the present preliminary in vivo results, indicating that the LPHD nasal administration allows to obtain the DMF uptake in the cerebrospinal fluid of rats. Further extensive in vivo studies are necessary to fully characterize the potential improvement of DMF nose-to-brain delivery by this proposed formulation.

Conclusion

Lipid-polymeric hybrid nanoparticles for DMF delivery were prepared using a straightforward and rapid method that facilitates easy scale-up. HA imparts to LPHD features suitable for IN administration by increasing viscosity, mucoadhesion, and providing protection of DMF from degradation. Nanoparticles promote DFM permeability and its intracellular transport through epithelial and neuronal cells, allowing to promote the nose-to-brain transport of DMF in rats. Therefore, HA-based lipid-polymeric nanoparticles hold significant promise as novel carriers for the *IN* administration of DMF in the treatment of multiple sclerosis.

Acknowledgments

This work was supported by the Foundation of Sardinia (Bando Fondazione di Sardegna 2018-2020 e 2021 – Progetti di ricerca di base dipartimentali; Grant numbers J89J21015120005), and by Autonomous Region of Sardinia (Legge Regionale 7 agosto 2007, n. 7 “Promozione della Ricerca Scientifica e dell’Innovazione Tecnologica in Sardegna”, Programma Mobilità Giovani Ricercatori - annualità 2022). This research was also supported by CNR project FOE-2021 DBA.AD005.225 and PRIN 2022 PNRR P2022RLH39 to SC. LAMEST Labs of the National Research Council performed morphological analyses. The authors thank Dr Flavia Lo Passo, Dr Giuseppina Zampi and Dr Fabio Gaeta (IBBR-CNR, Naples, Italy) for technical assistance, Ms Maria Rosaria Marcedula for the technical support in thermal

characterization of materials, and Maria Cristina del Barone for the technical support in TEM analyses. Special thanks to Dr Mattia Langellotto for helping in the creation of the graphical abstract.

Disclosure

The authors report no conflicts of interest in this work. The graphical abstract was created using BioRender software. Langellotto, M. (2024) https://BioRender.com/i91f605.

References

1. Rodríguez Murúa S, Farez MF, Quintana FJ. The immune response in multiple sclerosis. *Annu Rev Pathol Mech Dis*. 2022;17(1):121–139. doi:10.1146/annurev-pathol-052920-040318
2. Higuera L, Carlin CS, Anderson S. Adherence to disease-modifying therapies for multiple sclerosis. *J Manag Care Spec Pharm*. 2016;22 (12):1394–1401. doi:10.18553/jmcp.2016.22.12.1394
3. Waubant E, Lucas R, Mowry E, et al. Environmental and genetic risk factors for MS: an integrated review. *Ann Clin Transl Neurol*. 2019;6 (9):1905–1922. doi:10.1002/acn3.50862
4. Garg N, Smith TW. An update on immunopathogenesis, diagnosis, and treatment of multiple sclerosis. *Brain Behav*. 2015;5(9):e00362. doi:10.1002/brb3.362
5. Lategan TW, Wang L, Sprague TN, Rousseau FS. Pharmacokinetics and bioavailability of monomethyl fumarate following a single oral dose of bafiertam™ (Monomethyl Fumarate) or Tecfidera® (Dimethyl Fumarate). *CNS Drugs*. 2021;35(5):567–574. doi:10.1007/s40263-021-00799-9
6. Yazdi MR, Mrowietz U. Fumaric acid esters. *Clin Dermatol*. 2008;26(5):522–526. doi:10.1016/j.clindermatol.2008.07.001
7. Gold R, Arnold DL, Bar-Or A, et al. Long-term safety and efficacy of dimethyl fumarate for up to 13 years in patients with relapsing-remitting multiple sclerosis: final ENDORSE study results. *Mult Scler J*. 2022;28(5):801–816. doi:10.1177/13524585211037909
8. De La Maza SS, Sabin Muñoz J, De La Fuente BP, et al. Early predictive risk factors for dimethyl fumarate-associated lymphopenia in patients with multiple sclerosis. *Mult Scler Relat Disord*. 2022;59:103669. doi:10.1016/j.msard.2022.103669
9. Ojha S, Kumar B. Preparation and statistical modeling of solid lipid nanoparticles of dimethyl fumarate for better management of multiple sclerosis. *Adv Pharm Bull*. 2018;8(2):225–233. doi:10.15171/apb.2018.027
10. Kumar P, Sharma G, Kumar R, et al. Enhanced brain delivery of dimethyl fumarate employing tocopherol-acetate-based nanolipidic carriers: evidence from pharmacokinetic, biodistribution, and cellular uptake studies. *ACS Chem Neurosci*. 2017;8(4):860–865. doi:10.1021/acschemneuro.6b00428
11. Royaei M, Tahoori MT, Bardania H, Shams A, Dehghan A. Amelioration of inflammation through reduction of oxidative stress in rheumatoid arthritis by treating fibroblast-like synoviocytes (FLS) with DMF-loaded PLGA nanoparticles. *Int Immunopharmacol*. 2024;129:111617. doi:10.1016/j.intimp.2024.111617
12. Ojha S, Kumar B, Chadha H. Neuroprotective potential of dimethyl fumarate-loaded polymeric nanoparticles against multiple sclerosis. *Indian J Pharm Sci*. 2019;81(3). doi:10.36468/pharmaceutical-sciences.535
13. Rolfsen Ferreira Da Silva GB, Das Neves S P, Roque Oliveira SC, et al. Comparative effectiveness of preventive treatment with dimethyl fumarate-loaded solid lipid nanoparticles and oral dimethyl fumarate in a mouse model of multiple sclerosis. *J Autoimmun*. 2022;132:102893. doi:10.1016/j.jaut.2022.102893
14. Clementino AR, Pellegrini G, Banella S, et al. Structure and fate of nanoparticles designed for the nasal delivery of poorly soluble drugs. *Mol Pharm*. 2021;18(8):3132–3146. doi:10.1021/acs.molpharmaceut.1c00366
15. Linker RA, Gold R. Dimethyl fumarate for treatment of multiple sclerosis: mechanism of action, effectiveness, and side effects. *Curr Neurol Neurosci Rep*. 2013;13(11):394. doi:10.1007/s11910-013-0394-8
16. Kumar N, Khurana B, Arora D. Nose-to-brain drug delivery for the treatment of glioblastoma multiforme: nanotechnological interventions. *Pharm Dev Technol*. 2023;28(10):1032–1047. doi:10.1080/10837450.2023.2285506
17. Bourganis V, Kammona O, Alexopoulos A, Kiparissides C. Recent advances in carrier mediated nose-to-brain delivery of pharmaceutics. *Eur J Pharm Biopharm*. 2018;128:337–362. doi:10.1016/j.ejpb.2018.05.009
18. Borrajo ML, Alonso MJ. Using nanotechnology to deliver biomolecules from nose to brain — peptides, proteins, monoclonal antibodies and RNA. *Drug Deliv Transl Res*. 2022;12(4):862–880. doi:10.1007/s13346-021-01086-2
19. Mu H, Holm R, Müllertz A. Lipid-based formulations for oral administration of poorly water-soluble drugs. *Int J Pharm*. 2013;453(1):215–224. doi:10.1016/j.ijpharm.2013.03.054
20. Peer D, Karp JM, Hong S, Farokhzad OC, Margalit R, Langer R. Nanocarriers as an emerging platform for cancer therapy. *Nat Nanotechnol*. 2007;2(12):751–760. doi:10.1038/nnano.2007.387
21. Torchilin VP. Recent advances with liposomes as pharmaceutical carriers. *Nat Rev Drug Discov*. 2005;4(2):145–160. doi:10.1038/nrd1632
22. Hadinoto K, Sundaresan A, Cheow WS. Lipid–polymer hybrid nanoparticles as a new generation therapeutic delivery platform: a review. *Eur J Pharm Biopharm*. 2013;85(3):427–443. doi:10.1016/j.ejpb.2013.07.002
23. Owensiii D, Opsonization PN. biodistribution, and pharmacokinetics of polymeric nanoparticles. *Int J Pharm*. 2006;307(1):93–102. doi:10.1016/j.ijpharm.2005.10.010
24. Gabizon A, Amitay Y, Tzemach D, Gorin J, Shmeeda H, Zalipsky S. Therapeutic efficacy of a lipid-based prodrug of mitomycin C in pegylated liposomes: studies with human gastro-entero-pancreatic ectopic tumor models. *J Control Release*. 2012;160(2):245–253. doi:10.1016/j.jconrel.2011.11.019
25. Mohanty A, Uthaman S, Park IK. Utilization of polymer-lipid hybrid nanoparticles for targeted anti-cancer therapy. *Molecules*. 2020;25(19):4377. doi:10.3390/molecules25194377
26. Loría F, Petrosino S, Mestre L, et al. Study of the regulation of the endocannabinoid system in a virus model of multiple sclerosis reveals a therapeutic effect of palmitoylethanolamide. *Eur J Neurosci*. 2008;28(4):633–641. doi:10.1111/j.1460-9568.2008.06377.x

27. Giarra S, Serri C, Russo L, et al. Spontaneous arrangement of a tumor targeting hyaluronic acid shell on irinotecan loaded PLGA nanoparticles. *Carbohydr Polym*. 2016;140:400–407. doi:10.1016/j.carbpol.2015.12.031
28. Serri C, Frigione M, Ruponen M, et al. Electron dispersive X-ray spectroscopy and degradation properties of hyaluronic acid decorated microparticles. *Colloids Surf B Biointerfaces*. 2019;181:896–901. doi:10.1016/j.colsurfb.2019.06.044
29. Laffleur F, Hörmann N, Gust R, Ganner A. Synthesis, characterization and evaluation of hyaluronic acid-based polymers for nasal delivery. *Int J Pharm*. 2023;631:122496. doi:10.1016/j.ijpharm.2022.122496
30. Salama HA, Mahmoud AA, Kamel AO, Abdel Hady M, Awad GAS. Phospholipid based colloidal poloxamer–nanocubic vesicles for brain targeting via the nasal route. *Colloids Surf B Biointerfaces*. 2012;100:146–154. doi:10.1016/j.colsurfb.2012.05.010
31. Vasvani S, Kulkarni P, Rawtani D. Hyaluronic acid: a review on its biology, aspects of drug delivery, route of administrations and a special emphasis on its approved marketed products and recent clinical studies. *Int J Biol Macromol*. 2020;151:1012–1029. doi:10.1016/j.ijbiomac.2019.11.066
32. Mercier C, Perek N, Delavenne X. Is RPMI 2650 a suitable in vitro nasal model for drug transport studies? *Eur J Drug Metab Pharmacokinet*. 2018;43(1):13–24. doi:10.1007/s13318-017-0426-x
33. Krishna A, Biryukov M, Trefois C, et al. Systems genomics evaluation of the SH-SY5Y neuroblastoma cell line as a model for Parkinson's disease. *BMC Genomics*. 2014;15(1):1154. doi:10.1186/1471-2164-15-1154
34. Serri C, Argirò M, Piras L, et al. Nano-precipitated curcumin loaded particles: effect of carrier size and drug complexation with (2-hydroxypropyl)-β-cyclodextrin on their biological performances. *Int J Pharm*. 2017;520(1–2):21–28. doi:10.1016/j.ijpharm.2017.01.049
35. Juliano C, Cossu M, Pigozzi P, Rassu G, Preparation GP. In vitro characterization and preliminary in vivo evaluation of buccal polymeric films containing chlorhexidine. *AAPS Pharm Sci Tech*. 2008;9(4):1153–1158. doi:10.1208/s12249-008-9153-6
36. Lombardo R, Ruponen M, Rautio J, et al. A technological comparison of freeze-dried poly-ε-caprolactone (PCL) and poly (lactic-co-glycolic acid) (PLGA) nanoparticles loaded with clozapine for nose-to-brain delivery. *J Drug Deliv Sci Technol*. 2024;93:105419. doi:10.1016/j.jddst.2024.105419
37. Habib AA, Hammad SF, Amer MM, Kamal AH. Stability indicating RP-HPLC method for determination of dimethyl fumarate in presence of its main degradation products: application to degradation kinetics. *J Sep Sci*. 2021;44(3):726–734. doi:10.1002/jssc.202001007
38. Demartis S, Rassu G, Murgia S, Casula L, Giunchedi P, Gavini E. Improving dermal delivery of rose bengal by deformable lipid nanovesicles for topical treatment of melanoma. *Mol Pharm*. 2021;18(11):4046–4057. doi:10.1021/acs.molpharmaceut.1c00468
39. Di Cagno M, Bibi HA, Bauer-Brandl A. New biomimetic barrier permeapad^{tm} for efficient investigation of passive permeability of drugs. *Eur J Pharm Sci*. 2015;73:29–34. doi:10.1016/j.ejps.2015.03.019
40. Jacobsen AC, Visentin S, Butnarasu C, Stein PC, Di Cagno MP. Commercially available cell-free permeability tests for industrial drug development: increased sustainability through reduction of in vivo studies. *Pharmaceutics*. 2023;15(2):592. doi:10.3390/pharmaceutics15020592
41. Den Berg MP V, Romeijn SG, Verhoef JC, Merkus FWHM. Serial cerebrospinal fluid sampling in a rat model to study drug uptake from the nasal cavity. *J Neurosci Methods*. 2002;116(1):99–107. doi:10.1016/S0165-0270(02)00033-X
42. Dalpiaz A, Ferraro L, Perrone D, et al. Brain uptake of a zidovudine prodrug after nasal administration of solid lipid microparticles. *Mol Pharm*. 2014;11(5):1550–1561. doi:10.1021/mp400735c
43. Felgenhauer K. Protein size and cerebrospinal fluid composition. *Klin Wochenschr*. 1974;52(24):1158–1164. doi:10.1007/BF01466734
44. Madu A, Cioffe C, Mian U, et al. Pharmacokinetics of fluconazole in cerebrospinal fluid and serum of rabbits: validation of an animal model used to measure drug concentrations in cerebrospinal fluid. *Antimicrob Agents Chemother*. 1994;38(9):2111–2115. doi:10.1128/AAC.38.9.2111
45. Pinto BF, Ribeiro LNB, Da Silva GBRF, et al. Inhalation of dimethyl fumarate-encapsulated solid lipid nanoparticles attenuate clinical signs of experimental autoimmune encephalomyelitis and pulmonary inflammatory dysfunction in mice. *Clin Sci*. 2022;136(1):81–101. doi:10.1042/CS20210792
46. Keller LA, Merkel O, Popp A. Intranasal drug delivery: opportunities and toxicologic challenges during drug development. *Drug Deliv Transl Res*. 2022;12(4):735–757. doi:10.1007/s13346-020-00891-5
47. Lofts A, Abu-Hijleh F, Rigg N, Mishra RK, Hoare T. Using the intranasal route to administer drugs to treat neurological and psychiatric illnesses: rationale, successes, and future needs. *CNS Drugs*. 2022;36(7):739–770. doi:10.1007/s40263-022-00930-4
48. Esposito E, Cortesi R, Drechsler M, et al. Nanoformulations for dimethyl fumarate: physicochemical characterization and in vitro / in vivo behavior. *Eur J Pharm Biopharm*. 2017;115:285–296. doi:10.1016/j.ejpb.2017.04.011
49. Zeng W, Li Q, Wan T, et al. Hyaluronic acid-coated niosomes facilitate tacrolimus ocular delivery: mucoadhesion, precorneal retention, aqueous humor pharmacokinetics, and transcorneal permeability. *Colloids Surf B Biointerfaces*. 2016;141:28–35. doi:10.1016/j.colsurfb.2016.01.014
50. Ghosh P, Hutadilok N, Adam N, Lentini A. Interactions of hyaluronan (hyaluronic acid) with phospholipids as determined by gel permeation chromatography, multi-angle laser-light-scattering photometry and 1H-NMR spectroscopy. *Int J Biol Macromol*. 1994;16(5):237–244. doi:10.1016/0141-8130(94)90028-0
51. Della Sala F, Silvestri T, Borzacchiello A, Mayol L, Ambrosio L, Biondi M. Hyaluronan-coated nanoparticles for active tumor targeting: influence of polysaccharide molecular weight on cell uptake. *Colloids Surf B Biointerfaces*. 2022;210:112240. doi:10.1016/j.colsurfb.2021.112240
52. Snetkov P, Zakharova K, Morozkina S, Olekhnovich R, Uspenskaya M. Hyaluronic acid: the influence of molecular weight on structural, physical, physico-chemical, and degradable properties of biopolymer. *Polymers*. 2020;12(8):1800. doi:10.3390/polym12081800
53. Wu L, Zhang J, Watanabe W. Physical and chemical stability of drug nanoparticles. *Adv Drug Deliv Rev*. 2011;63(6):456–469. doi:10.1016/j.addr.2011.02.001
54. Kovacevic A, Savic S, Vuleta G, Müller RH, Keck CM. Polyhydroxy surfactants for the formulation of lipid nanoparticles (SLN and NLC): effects on size, physical stability and particle matrix structure. *Int J Pharm*. 2011;406(1–2):163–172. doi:10.1016/j.ijpharm.2010.12.036
55. Cama ES, Catenacci L, Perteghella S, et al. Design and development of a chitosan-based nasal powder of dimethyl fumarate-cyclodextrin binary systems aimed at nose-to-brain administration. A stability study. *Int J Pharm*. 2024;659:124216. doi:10.1016/j.ijpharm.2024.124216
56. Horvát S, Fehér A, Wolburg H, et al. Sodium hyaluronate as a mucoadhesive component in nasal formulation enhances delivery of molecules to brain tissue. *Eur J Pharm Biopharm*. 2009;72(1):252–259. doi:10.1016/j.ejpb.2008.10.009
57. Morimoto K, Yamaguchi H, Iwakura Y, Morisaka K, Ohashi Y, Nakai Y. No title found. *Pharm Res*. 1991;08(4):471–474. doi:10.1023/A:1015894910416

58. Guidance for industry. nasal spray and inhalation solution, suspension, and spray drug products - chemistry, manufacturing, and controls documentation; 2002. Available from: https://www.fda.gov/files/drugs/published/Nasal-Spray-and-Inhalation-Solution–Suspension–and-Drug-Products.pdf. Accessed December 21, 2024.
59. Kulkarni V, Shaw C Formulation and characterization of nasal sprays. Inhalation; 2012; Available from: https://www.inhalationmag.com/wp-content/uploads/pdf/inh_20120601_0010.pdf. Accessed December 21, 2024.
60. Mayol L, Quaglia F, Borzacchiello A, Ambrosio L, Rotonda M. A novel poloxamers/hyaluronic acid in situ forming hydrogel for drug delivery: rheological, mucoadhesive and in vitro release properties. *Eur J Pharm Biopharm*. 2008;70(1):199–206. doi:10.1016/j.ejpb.2008.04.025
61. Oliveira Cardoso VM D, Gremião MPD, Cury BSF. Mucin-polysaccharide interactions: a rheological approach to evaluate the effect of pH on the mucoadhesive properties. *Int J Biol Macromol*. 2020;149:234–245. doi:10.1016/j.ijbiomac.2020.01.235
62. Sepulveda AF, De Araujo DR. Bioadhesive behavior of poloxamer/hyaluronic acid-based formulations analyzed by rheology method. *Sci Talks*. 2022;4:100072. doi:10.1016/j.sctalk.2022.100072
63. Di Cagno M, Luppi B. Drug "supersaturation" states induced by polymeric micelles and liposomes: a mechanistic investigation into permeability enhancements. *Eur J Pharm Sci*. 2013;48(4–5):775–780. doi:10.1016/j.ejps.2013.01.006
64. Mukherjee A, Waters AK, Kalyan P, Achrol AS, Kesari S, Yenugonda VM. Lipid–polymer hybrid nanoparticles as a next-generation drug delivery platform: state of the art, emerging technologies, and perspectives. *Int J Nanomed*. 2019;14:1937–1952. doi:10.2147/IJN.S198353